

## **Fluid-Structure Interactions of Physiological and Pulsatile Flow cases in Stenosed Artery**

**Taewon Seo**

*Department of Mechanical and Automotive Engineering  
Andong National University, Andong, 760-749 Korea,  
phone: 82-54-820-5756; fax: 82-54-820-5044; e-mail: [dongjin@anu.ac.kr](mailto:dongjin@anu.ac.kr)*

### **Abstract**

The objective of this study is to understand how the flow patterns and wall shear stress fields change with the development of stenosis by numerically analyzing the interactions between a blood flow and an arterial wall. Fluid-Structure Interaction (FSI) model becomes essential to achieve a basic understanding of effects of various mechanical forces involved in arterial disease development. The present study is concerned with physiological and pulsatile flow cases in elastic wall vessels with 25, 50 and 75% constriction of cross-sectional areas in stenosed arteries. In the study, shear stresses along the wall, velocity field and wall motions are discussed in the different type of constriction of the blood vessel under the physiological and pulsatile flow conditions. Comparison results between physiological and pulsatile flow cases show that the flow characteristic of physiological flow is slightly higher at some instances of time. Results obtained may provide useful information for early detection, prevention and diagnosis of related arterial disease.

**Keywords:** Stenosis, Atherosclerosis, Fluid-Structure Interaction, Physiological flow, Pulsatile flow, Stenosed Artery.

## Introduction

Atherosclerosis is a disease of large- and medium-size arteries in which localized deposits and accumulation of cholesterol and lipid substances as well as proliferation of connective tissues cause a partial reduction in the arterial cross-sectional area (stenosis). Development of atherosclerosis, even in the early stages of the disease, is strongly related to the characteristics of the blood flow in the arteries.<sup>1,2)</sup> The symptom of atherosclerotic cardiovascular disease is heart attack or sudden cardiac death. The most artery flow disrupting events occur at locations with less than 50% of lumen narrowing (~20% stenosis is average).<sup>3)</sup> According to cardiac stress testing, traditionally the most commonly performed non-invasive testing method for blood flow limitations generally only detects lumen narrowing of ~75% or greater.

From clinical trials, 20% is the average stenosis at plaques that subsequently rupture with resulting complete artery closure. Most severe clinical events do not occur at plaques that produce high-grade stenosis.<sup>4)</sup> Only 14% of heart attacks occur from artery closure at plaques producing 75% or greater stenosis prior to the vessel closing.

A considerable numbers of experimental and numerical research works have been conducted to study the flow dynamics and stresses in elastic collapsible tube.<sup>5,6,7,8)</sup> Although a large number of investigations have led to better understanding of the flow disturbances induced by a stenosis, most of the theoretical and experimental studies have been performed under different simplifying assumptions.

In most of the studies, flow has been assumed axisymmetric.<sup>9,10,11,12)</sup> Some studies have considered the wall to be rigid<sup>9)</sup> and elastic.<sup>11,13)</sup> Some assumed flow to be laminar,<sup>9,11,12)</sup> and some focused on steady or unsteady flow with constant inlet velocity and outlet pressure conditions.<sup>9,10,12,13,14)</sup> For example, Tang<sup>15)</sup> used axisymmetric models to investigate steady or unsteady viscous flow in elastic stenotic tubes with various stenosis stiffness and pressure conditions. Cavalcanti<sup>20)</sup> did numerical simulation to examine the hemodynamics in a mild stenosis with consideration of pulsatile wall motion. Sarifuddin<sup>18)</sup> used computational methods to investigate the interaction between fluid mechanics and the artery wall. Bathe<sup>19)</sup> introduced an axisymmetric thick-wall model with fluid structure interactions for pulsatile blood flow through a compliant stenotic artery. Lee<sup>11)</sup> et al. used axisymmetrically 45% stenosed model under the unsteady pulsatile flow condition and presented comparisons between rigid and compliant models. Their comparison results were qualitatively similar but considerable difference in magnitude. Zendehebudi<sup>9)</sup> et al.

considered laminar flow and axisymmetric 56% rigid stenosis under the steady flow case. He compared physiological flow with simple pulsatile flow. Comparisons of their results showed that the behavior of the two flows were similar at some instances of time. Tang<sup>15)</sup> et al. considered steady flow through an axisymmetric stenotic vessel using the commercial code ADINA. They observed complex flow patterns and high shear stresses at the throat of the stenosis, as well as compressive stresses inside the tube. Buchanan<sup>20)</sup> studied rheological effects on pulsatile laminar flow through an axisymmetric stenosed tube and found that they could affect wall shear stress quantities. Yamaguchi<sup>21)</sup> et al. considered fluid-structure interactions in the collapse and ablation of atheromatous plaque in coronary arteries and found that wall shear stress distribution has very localized pattern and that the dragging force from fluid has a considerable effect on wall compression under physiological conditions. Powell<sup>22)</sup> measured the tube law for bovine carotid artery and studied the effects of severity of stenosis. Their results showed that the tube wall collapsed under physiological conditions.

The present study is concerned with physiological and pulsatile flows in elastic wall vessels with 25, 50 and 75% constriction of cross-sectional area in stenosed arteries. The objective of this study is to understand how the flow features and wall shear stress field change with the development of stenosis by numerically analyzing the interactions between a blood flow and a stenosed wall. In this present study, comparisons of shear stresses along the wall, velocity field and wall motion are discussed in the different type of constriction of the blood vessel under the physiological and pulsatile flow conditions.

## 2. Formulation of the Problem

### 2.1 Geometric Model of Blood Vessel

The diseased artery was modeled as an axisymmetric stenosis with 25%, 50% and 75% area reductions, respectively in Fig. 1. FSI model is considered with incorporating the fluid-wall interaction under the physiological and pulsatile flow conditions with an elastic wall. As shown in Fig. 1, the total length of the geometry of a cylindrical tube adopted is  $24D$ , where  $D=0.004\text{m}$  is the diameter of the non-stenosed region of the artery. Entrance length of the blood flow to stenosis region is  $2D$ .  $t_1$ ,  $t_2$ ,  $t_3$  are assumed stenotic rates in the model, respectively. The length of the stenosis is  $2D$ . Thickness of the blood vessel wall is assumed to be  $D/4$ .

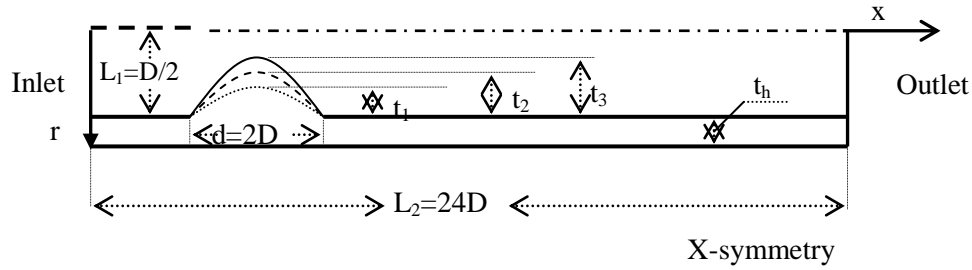


**Fig. 1 Schematic geometry of the stenosed blood vessel with elastic wall model (FSI Model)**

## **2.2 Flow Modeling**

We consider viscous flow in a compliant vessel simulating blood flow in stenotic arteries. The blood is assumed to be incompressible, laminar and Newtonian, while the wall is isotropic and elastic.

The governing equations for the conservation of mass and momentum of an incompressible and Newtonian fluid are the axisymmetric, time-dependent Navier-Stokes equations, which are shown as follows:

- Continuity equation

$$\frac{\partial u}{\partial x} + \frac{\partial v}{\partial r} + \frac{v}{r} = 0 \quad (1)$$

- Momentum equation in the axial direction

$$\frac{\partial u}{\partial t} + u \frac{\partial u}{\partial x} + v \frac{\partial u}{\partial r} = -\frac{1}{\rho} \frac{\partial p}{\partial x} + \nu \left( \frac{\partial^2 u}{\partial r^2} + \frac{1}{r} \frac{\partial u}{\partial r} + \frac{\partial^2 u}{\partial x^2} \right) \quad (2)$$

- Momentum equation in the radial direction

$$\frac{\partial v}{\partial t} + u \frac{\partial v}{\partial x} + v \frac{\partial v}{\partial r} = -\frac{1}{\rho} + \nu \left( \frac{\partial^2 v}{\partial r^2} + \frac{1}{r} \frac{\partial v}{\partial r} + \frac{\partial^2 v}{\partial x^2} - \frac{v}{r^2} \right) \quad (3)$$

where  $u$  and  $v$  are the axial and radial components of the blood velocities,  $\rho$  is the blood density and  $\nu$  is the kinematic viscosity.

The stress tensor in the Cartesian tensor notation is defined below:

$$\begin{aligned}\sigma_{ij} &= -p\delta_{ij} + \tau_{ij} \\ \tau_{ij} &= 2\mu\varepsilon_{ij} \\ \varepsilon_{ij} &= \frac{1}{2}\left(\frac{\partial u_i}{\partial x_j} + \frac{\partial u_j}{\partial x_i}\right)\end{aligned}\tag{4}$$

where  $\delta_{ij}$  is the Kronecker delta,  $\tau_{ij}$  are the components of the shear stress tensor,  $\varepsilon_{ij}$  are the components of rate of deformation tensor,  $\mu$  is the dynamic viscosity of the fluid and  $i, j$  represent the axial and radial direction, respectively.

### **2.3 Wall Modeling**

The stenotic wall is considered to be isotropic and elastic with Young's modulus  $E=0.7\times 10^6$  (N/m<sup>2</sup>), Poisson's ratio  $\nu=0.49$  and density of blood vessel wall  $\rho_s=2000$ (kg/m<sup>3</sup>). The blood vessel wall thickness is uniform at 1mm in normal region and the maximum thickness at the throat of the stenotic region is 2.5mm.

The motion of an elastic vessel wall is mathematically described by the equation shown below:

$$\rho_s \frac{\partial^2 d_i}{\partial t^2} = \frac{\partial \sigma_{ij}}{\partial x_j}, \text{ for } i, j=x, r\tag{5}$$

where  $\rho_s$  is the vessel wall density,  $d_i$  are the components of the wall displacements and  $\sigma_{ij}$  are the components of the wall stress tensor. The stress tensor  $\sigma_{ij}$  is obtained from the constitutive equation of the material, and it can be expressed for a Hookean elastic wall as:

$$\sigma_{ij} = \lambda_L e_{kk} \delta_{ij} + 2\mu_L e_{ij}\tag{6}$$

where  $\lambda_L$  and  $\mu_L$  are the Lamé constants and  $e_{ij}$  are the components of the strain tensor in the solid.

The conditions of displacement compatibility and traction equilibrium along the fluid-structure interface are satisfied:

- Displacement Compatibility

$$\vec{d}_f = \vec{d}_s \quad (7)$$

- Traction Equilibrium

$$\vec{f}_f = \vec{f}_s \quad (8)$$

where  $\vec{d}$  and  $\vec{f}$  are displacement and tractions and the subscripts  $f$  and  $s$  stand for fluid and solid respectively.

#### **2.4 Boundary Conditions and Numerical Method**

The physiological flow at the inlet is specified by the temporal waveform given by Zendehbudi<sup>9)</sup> in the canine femoral artery as shown in Fig. 2(a). In this study the mean velocity,  $\bar{U} = 0.33 \text{ m/s}$ , corresponding to  $\text{Re} = 400$  is applied. The maximum velocity in Fig. 2 is  $0.66 \text{ m/s}$ . The inlet velocity initially accelerates and reaches a maximum of  $0.99 \text{ m/sec}$  at  $t = 0.16$ . After this point the velocity magnitude begins to decrease and drops to  $-0.28 \text{ m/sec}$  at  $t = 0.42$ . In this study, five different times corresponding to the conditions of accelerating point (A), peak forward (B), decelerating point (C) and peak backward (D, E) were observed every cycle.

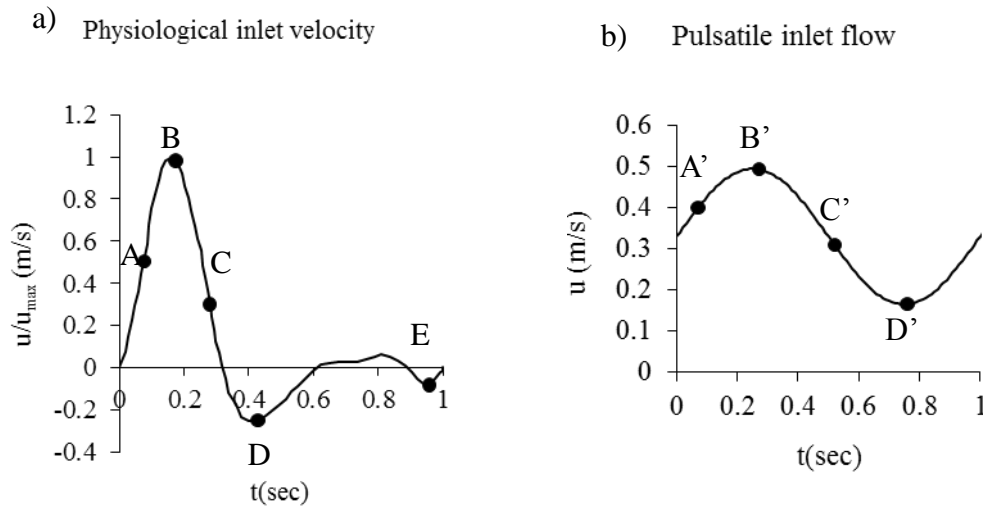


**Fig. 2 Time variations of mean velocities for physiological<sup>9)</sup> and sinusoidal pulsatile flows.**

No-slip velocity conditions are imposed on the arterial wall. At the outlet, flow satisfies zero pressure flow conditions. On the axis of symmetry the axial velocity gradient and cross flow will be zero ( $\frac{\partial u}{\partial r} = v = 0$  at  $r=0$ ).

For the pulsatile flow simulations, the inlet velocity is assumed to be uniform with a sinusoidal temporal waveform (Fig. 2(b))

$$u = U_m (1 + \sin 2\pi t) \quad (9)$$

At the outlet, flow satisfies the fully developed flow conditions. The length of the geometry was chosen to be sufficiently long to satisfy this outlet condition. A no-slip condition is imposed at the wall. The simulations were performed to various flow parameters in order to assess the sensitivity of the flow field. Inlet velocity profiles are uniform, parabolic and the pulsatile flow and the Reynolds numbers of 400. In this study four distinct times corresponding to the conditions of accelerating point (A'), peak forward (B'), decelerating point (C') and peak backward (D') were investigated.

The governing equations were solved using finite element commercial computational fluid dynamic software ADINA (version 8.4, ADINA, Watertown, MA). ADINA fluid-structure interaction code is developed to apply for fully coupled

analysis of fluid flow with structural interaction problem. To solve the fluid equations coupled with solid equations ADINA is employed in this study.

Fluid flow was solved by applying the direct solution method with applied 0.8 relaxing force and displacement. Meshing was composed of Rule-Based meshing method which is a Structural Meshing Algorithm. Simulation results were assumed to be independent of the computational mesh when the disparity between meshes of varying densities was less than 5%. The Newton Method has been adopted as the iterative algorithm in all simulations. Maximum iteration repeated 15 times in order to in one step and allowable error was  $10^{-5}$ . Time periodic solutions were typically obtained after 3 cycles and were defined when the cycle average difference in the size of the recirculation zone in the vicinity of the stenotic region fell below 5%.

All the computations were performed on an Intel Pentium IV 3.19 GHz with 3.5 GB RAM operating Windows XP. The computational solving process under the physiological inlet flow conditions took approximately 4 hours CPU time and several days CPU took for pulsatile inlet flow cases.

### **3. Results and Discussion**

#### **3.1 Model Validation**

Unsteady wall shear stress and of other hemodynamic variables were studied with experimental data by Lee<sup>11)</sup>*et al.* In our earlier study<sup>6,7)</sup>, our computed results were compared with Lee's data to validate the numerical method and computer code. Comparisons results between ours and Lee's data indicated good agreement.

The numerical model of blood flow was carried out with the mesh independence in Fig. 3 at the location  $x' (=x/D) =1$ , where  $x'$  is the normalized distance from the center of the stenosis.  $D$  is the inlet diameter of the blood vessel and  $x$  is the axial distance away from the center of the stenosis as shown in Fig. 1. As shown in Fig. 4, the meshes used for all simulations in this study ranged from 62,400 to 67,200 nodes to verify all solutions. Time-periodic physiological and pulsatile flow solutions were typically obtained after 3 cycles.



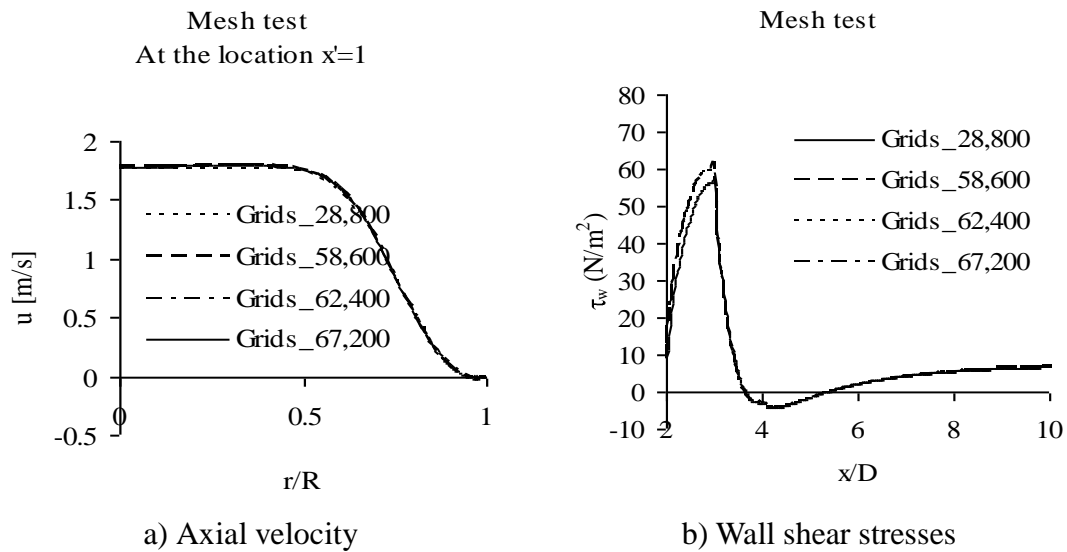


**Fig. 3 Axial velocities at  $x'=1$  and wall shear stresses along the vessel wall for 4 different number of meshes**

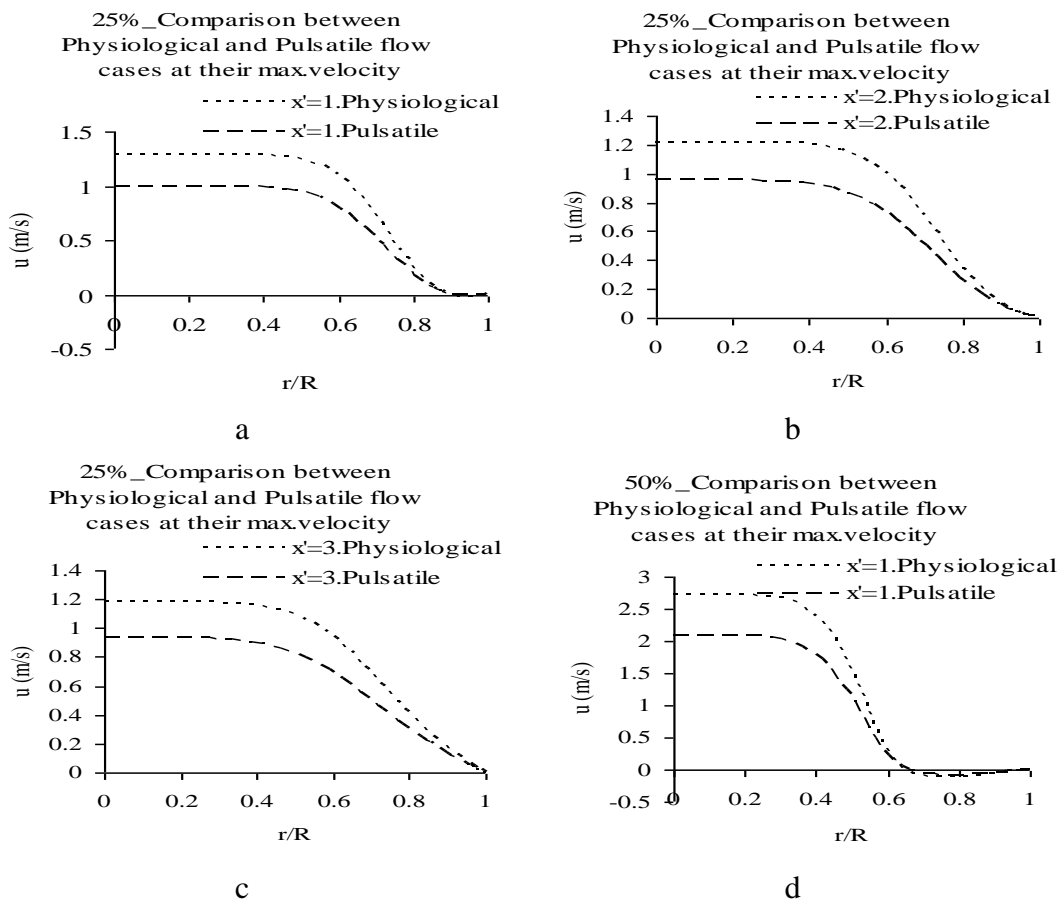
### 3.2. Comparison between physiological and pulsatile flow cases

#### 3.2.1 Comparison of velocity

The effects of wall compliance on flow patterns in the 25%, 50% and 75% axi-symmetrically stenosed blood vessel can be seen from the axial velocity profile results of the FSI model at different times of the cycle in Fig. 4. Due to the temporal nature of the wall dilation, the inner wall position varied throughout the cycle, and hence, the size of the flow separation indicated by negative velocity region near the wall also changed with time at three different locations in the post-stenotic region  $x' = 1$ ,  $x' = 2$  and  $x' = 3$ , where  $x'$  is the normalized distance from the center of the stenosis.  $x'=x/D$ ,  $x$  is the axial distance away from the center of the stenosis and  $D$  is the inlet diameter of the tube (Fig. 1).

After getting results from physiological and pulsatile flow condition cases, these 2 conditions were compared at their reached maximum time at different stenosed rate cases in Fig.4. The feature of axial velocities at the center being higher in physiological flow condition was quite common for all three chosen locations. The reverse flow zone tended to be larger in physiological flow condition with comparing pulsatile flow condition.

When the flow rate reached its maximum, negative velocity near the wall was registered at all chosen position. However, for the 25% stenosed rate cases, no recirculation was found for both flow conditions at  $x' = 2$  and 3 in Fig.4 (b, c). Comparison results show that the highest velocity magnitude occurred at the 75% stenosed rate case under the physiological flow condition. Peak velocity magnitude was 1.27 (m/s) at 25% stenosed rate case for physiological flow condition at location  $x'=1$ . For pulsatile flow condition, peak velocity magnitude indicated 0.99 (m/s) at  $x'=1$ . In case of 50% stenosed rate cases, peak velocity magnitude was 2.70 m/s for physiological flow condition and 2.07 m/s for pulsatile flow condition at  $x'=1$ . Similarly, for 75% stenosed cases peak velocity magnitude for physiological flow condition was 2.81 m/s and 2.16 m/s for pulsatile flow condition at  $x'=1$ .



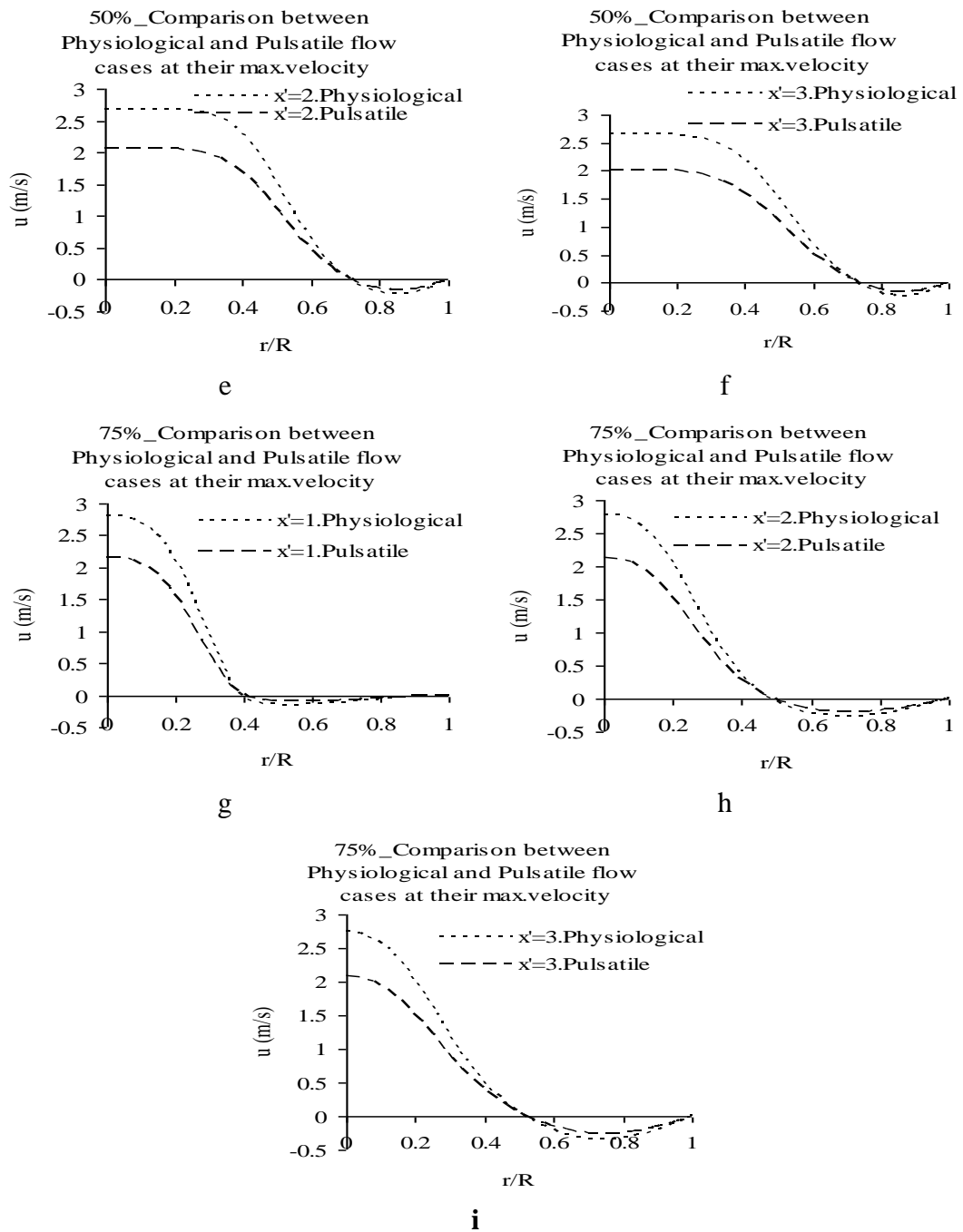


**Fig. 4** Comparisons between Physiological and Pulsatile flow cases at reached their maximum time at different stenosed rates cases.

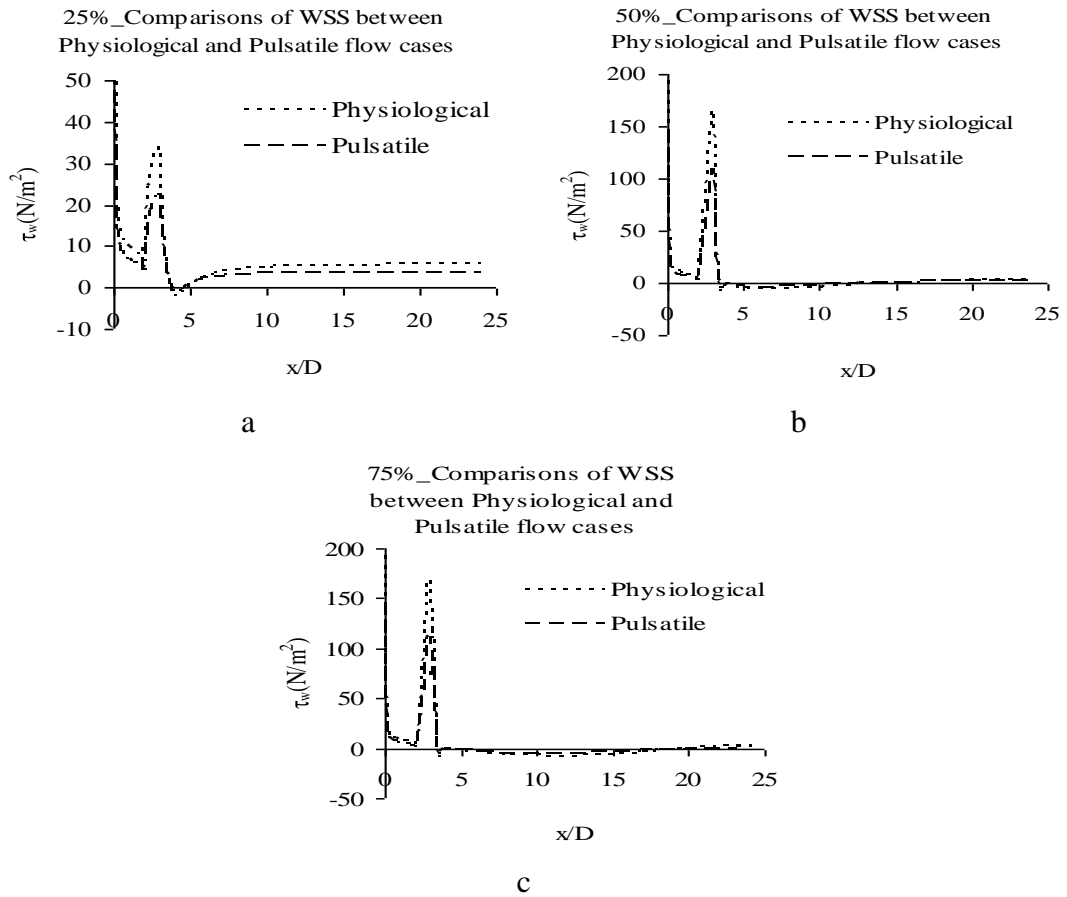
### 3.2.2 Comparison of wall shear stress

Fig. 5 shows comparisons of maximum reached wall shear stress distributions of physiological and pulsatile flow cases at along the axial direction. Maximum wall shear stress occurred at point B and B' at the throat of the stenosed region while minimum wall shear stress occurred at point D and D' in both cases. Furthermore, point C and C' indicated how the wall shear stress rapidly declined with time variation at 25%, 50% and 75% stenosed rate cases. In this study, comparisons hold only their reached maximum wall shear stress to understand behavior of these two flow cases.

Wall shear stress was higher in the pre-stenotic and stenotic regions in physiological flow condition. However this trend did not hold in the post-stenotic downstream as it varied with time and axial distance. Negative wall shear stress region, indicating the occupancy of flow reversal, grew axially longer significantly at 50% and 75% stenosed rate cases.

Peak wall shear stress was  $33.64 \text{ N/m}^2$  at 25% stenosed rate case for physiological flow condition. For pulsatile flow condition, peak wall shear stress indicated  $22.6 \text{ N/m}^2$ . In case of 50% stenosed cases, peak wall shear stress was  $165.57 \text{ N/m}^2$  for physiological flow and  $106.07 \text{ N/m}^2$  for pulsatile flow case. Similarly, for 75% stenosed cases peak wall shear stress for physiological flow was  $167.77 \text{ N/m}^2$  and  $110.43 \text{ N/m}^2$  for pulsatile flow case.

According to the clinical point of view, shear stress is more essential. When blood force distribution acts on the boundary surfaces of stenosed area, high shear stress occurs at throat section of stenosed area and rapidly drops reversing its direction. If the stenosed rate increases, high shear stress occurs at the vicinity of the stenosed area which means that blood flow could be closure or vessel wall could collapse because of high stenosed rate and high shear stress. Our results showed that the highest shear stress occurred at 50% and 75% stenosed rates cases, which could cause shutting down of blood supply. Fry<sup>17)</sup> said, shear stresses may severely damage endothelium cells, or even strip them from the vessel wall. Furthermore, according to the clinical trials, 20% is the average stenosis rate that subsequently ruptures with resulting complete artery closure.



**Fig. 5 Comparisons of wall shear stress distributions between physiological and pulsatile flow condition cases at their reached maximum time in different stenosed rates cases.**

**3.2.3 Comparison of wall displacement**

Fig. 6 shows plots of comparisons of maximum radial wall displacements with different stenosed rate cases under the 2 different flow cases. Inlet and outlet conditions were fixed at the solid part of FSI model by setting zero displacement. The wall model is constrained significantly for all the three rate cases at the stenosed region. The maximum radial wall displacement specifically stretched out at  $t = 0.16(B)$  at the stenosed area while minimum radial wall displacement lengthened at  $t = 0.42(D)$  in case of physiological flow case. For pulsatile flow case, maximum radial wall displacement stretched out at  $t = 0.25(B')$  while minimum radial wall displacement lengthened at  $t = 0.75(D')$ .

Our comparisons hold only maximum reached radial wall displacement of physiological and for pulsatile flow cases. Comparisons of radial wall displacements show that the maximum radial wall stretch occurred in physiological flow case at all stenosed rate cases. The smallest radial wall stretch was at 25% stenosed rate cases due to low curved area. The most axial wall stretch occurred at 75% stenosed rate case.

Radial wall stretch was higher and longer as general cases of 50% and 75% stenosed rate cases, and these cases can effect on blood artery, moreover, could collapse the artery.

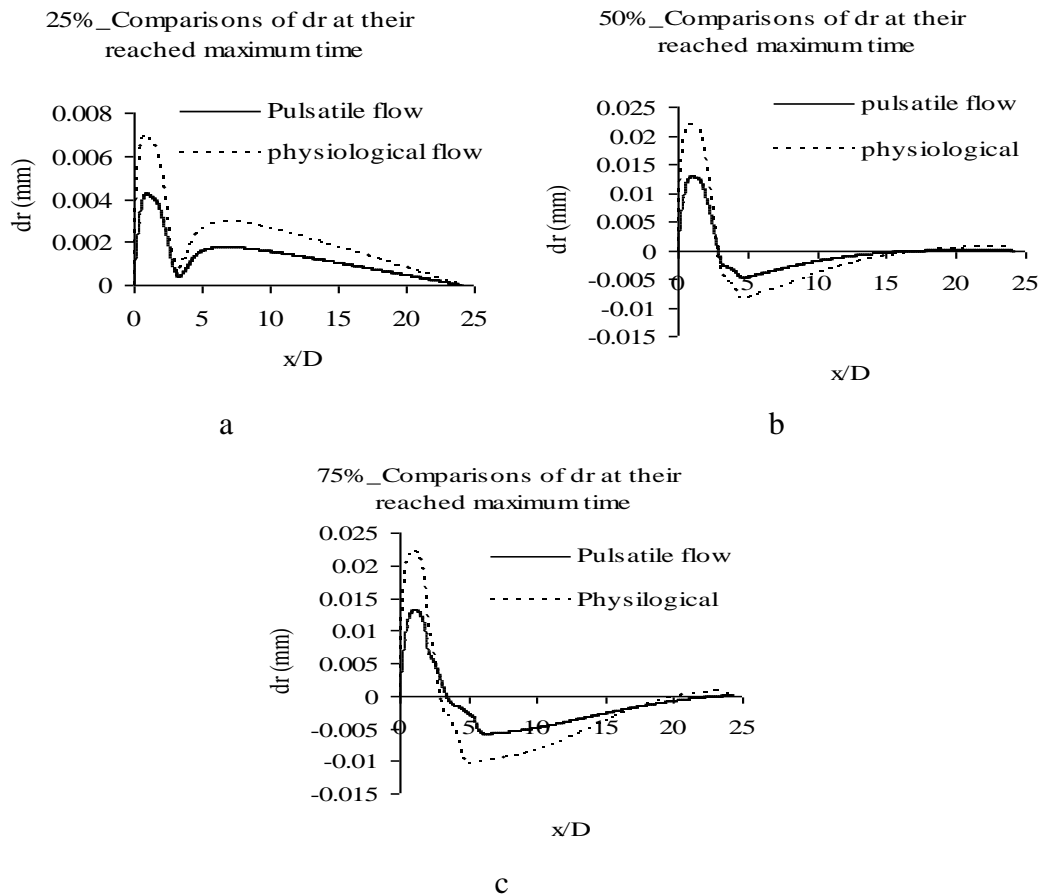


**Fig. 6 Comparison of radial wall displacement between physiological and pulsatile flow cases at their maximum reached time in different stenosed rates cases.**

## **5. Concluding Remarks**

In this research, Fluid – structure interaction model was accomplished under the physiological and pulsatile flow condition cases with time variation at 25%, 50% and 75% stenosed rate cases by using commercial CFD code, ADINA 8.4 program.

The fluid dynamics and vessel mechanical behavior were found to be an axisymmetric from the results for flow velocity, wall displacement and wall shear stress. The effects of Fluid – structure interaction model under the physiological and pulsatile flow cases on the stenosis were small at 25% stenosed rate case and did not change the fluid and solid behaviour significantly at 25% stenosed rate case. However, in case of 50% and 75% cases, the effects of physiological and pulsatile flow cases on the stenosis were higher which means blood flow could be closure or vessel wall could be collapsed because of high stenosed rate and high shear stress.

Wall shear stress was higher in the pre-stenotic and stenotic regions in the physiological flow condition. Negative wall shear stress region, indicating the occupancy of flow reversal, grew axially longer significantly at 50% and 75% stenosed rate cases. The feature of axial velocities at the center being higher in physiological flow condition was quite common for the three chosen locations with comparing pulsatile flow case and reverse flow zone tended to be thicker and longer in the stenosed region.

Comparisons of radial wall displacements indicated that the maximum radial wall stretch occurred in physiological flow case at all stenosed rate cases. Radial wall stretch was higher and longer as general cases of 50% and 75% stenosed rate cases, and these cases can effect on blood artery, moreover, could collapse the artery.

According to clinical point, hemodynamic factors play an important role on the localization of early atherosclerotic lesions. Our 50% and 75% stenosed rate cases could effect on blood artery due to hemodynamic factors (20% is the average stenosed rate). Our specific aim of this study was to understand the sensitivity of the computed flow cases to prescribed changes in geometric and parameters.

## **Acknowledgement**

The author was supported in part by the National Research Foundation (NRF) of Korea, (grant No. 2010-0021121).

**References:**

- [1] Steinman, D.A., 2004, Image-Based Computational Fluid Dynamics: A New Paradigm for Monitoring Hemodynamics and Atherosclerosis, *Curr. Drug Targets Cardiovasc.HaematolDisord.*, Jun;4(2), 183-197.
- [2] Lorenzini, G. and Casalena, E., 2008, CFD Analysis of Pulsatile Blood Flow in an Atherosclerotic Human Artery with Eccentric Plaques, *J. Biomech.*,41(9), 1862-1870.
- [3] Mol, A. 2002, *The Body Multiple: Ontology in Medical Practice*, London: Duke University Press
- [4] Wald, N.J. and Law, M.R., 2003, A Strategy to Reduce Cardiovascular Disease by more than 80%, *BMJ*, 326, 1419-1425.
- [5] Chan, W.Y., 2011, *Simulation of Arterial Stenosis Incorporating Fluid-Structural Interaction and Non-Newtonian Blood Flow*, RMIT Univ., Australia, Master Thesis.
- [6] Seo, T.W., 2013, Hemodynamic Characteristics in the Human Carotid Artery Model Induced by Blood-Arterial Wall Interaction, *WASET*, 7(5), 146-151.
- [7] Buriev, B., Kim, T.D. and Seo, T.W., 2009, Fluid-Structure Interactions of Physiological Flow in Stenosed Artery, *Korea-Australia Rheology J.*,21(1), 39-46.
- [8] Shaik, E., 2007, *Numerical Simulations of Blood Flow in Arteries using Fluid-Structure Interactions*, Wichita State Univ., PhD Dissertation
- [9] Zendehebudi, G.R. and Moayeri, M.S., 1999, Comparison of Physiological and Simple Pulsatile Flows through Stenosed Arteries, *Journal of Biomechanics*, 32, 959-965
- [10] Siegel, J.M. and Markou, C.P., 1994, A Scaling Law for Wall Shear Rate through an Arterial Stenosis, *Journal of Biomechanical Engineering Transaction ASME*, 116, 446-451
- [11] Lee, K.W. and Xu, X.Y., 2002, Modelling of Flow and Wall Behavior in a Mildly Stenosed Tube, *Medical Engineering & Physics*, 24, 575-586
- [12] Liao, W., Lee, T.S. and Low, H.T., 2004, Numerical Studies of Physiological Pulsatile Flow through Constricted Tube, *Inter. J. Numerical Methods for Heat & Fluid Flow*, 14(5), 689-713.



- [13] D. Tang, C. Yang, and D. N. Ku, 1999, A 3-D Thin-Wall Model with Fluid-Structure Interactions for Blood Flow in Carotid Arteries with Symmetric and Asymmetric Stenoses, *Computers and Structures*, 72, 357-377.
- [14] Mittal, M., Simmons, S.P., and Udaykumar, H.S., 2001, Application of Large-Eddy Simulation to the Study of Pulsatile Flow in a Modeled Arterial Stenosis, *Journal of Biomechanical Engineering Transaction ASME*, 123, 325-332.
- [15] Tang, D., Yang, J., Yang, C. and Ku, D.N., 1999, A Nonlinear Axisymmetric Model with Fluid-Wall Interactions for Steady Viscous Flow in Stenosed Elastic Tubes, *J. Biomech. Eng.*, 121(5), 494-501.
- [16] Peet, Y.V., Chopp, D.L., Davis, S.H. and Miksis, M.J., 2011, Computational Study of Unsteady Viscous Flow in Flexible Vessel, *Proceeding ASME June 22-25, Farmington, PA, USA*
- [17] Fry, D. L., 1972, "Response of the arterial wall to certain physical factors. atherogenesis: initiating factors," *A Ciba Foundation Symp.*, ASP, Amsterdam, The Netherlands, 40-83
- [18] Sarifuddin, C.S., Mandal, P.K. and Layek, G.C., 2008, Numerical Simulation of Unsteady Generalized Newtonian Blood Flow Through Differently Shaped Distensible Arterial Stenoses, *J. Med. Eng. & Tech.*, 32(5), 385-399.
- [19] Bathe, M., 1998, A fluid-structure interaction finite element analysis of pulsatile blood flow through a compliant stenotic artery, B. S. Thesis, MIT.
- [20] Buchanan, J.R., Kleinstreuer, C., and Comer, J.K., 2000, Rheological Effects on Pulsatile Hemodynamic in a Stenosed Tube, *Compute. Fluids*, 29, 695-724.
- [21] Yamaguchi, T., Kobayashi, T., and Liu, H., 1998, Fluid-Wall Interactions in the Collapse and Ablation of an Atheromatous Plaque in Coronary Arteries, *Proc. Third world congress of biomechanics*, p.20b.
- [22] Powell, B.E., 1991, Experimental measurements of Flow through stenotic collapsible tubes, M. S. Thesis, Georgia Inst. of Tech.

